

A novel *Staphylococcus aureus* cis–trans type I toxin–antitoxin module with dual effects on bacteria and host cells

Noëlla Germain-Amiot^{1,†}, Yoann Augagneur^{1,†}, Emilie Camberlein¹, Irène Nicolas¹, Valérie Lecqueur², Astrid Rouillon^{1,*} and Brice Felden^{1,*}

¹Université de Rennes 1, Inserm, BRM (Bacterial Regulatory RNAs and Medicine) UMR_S 1230, 35000 Rennes, France and ²Université de Rennes 1, CHU Rennes, Inserm, EHESP, Irset (Institut de recherche en santé, environnement et travail) UMR_S 1085, 35000 Rennes, France

Received August 03, 2018; Revised November 29, 2018; Editorial Decision November 30, 2018; Accepted December 05, 2018

ABSTRACT

Bacterial type I toxin–antitoxin (TA) systems are widespread, and consist of a stable toxic peptide whose expression is monitored by a labile RNA antitoxin. We characterized *Staphylococcus aureus* SprA2/SprA2_{AS} module, which shares nucleotide similarities with the SprA1/SprA1_{AS} TA system. We demonstrated that SprA2/SprA2_{AS} encodes a functional type I TA system, with the cis-encoded SprA2_{AS} antitoxin acting in trans to prevent ribosomal loading onto SprA2 RNA. We proved that both TA systems are distinct, with no cross-regulation between the antitoxins *in vitro* or *in vivo*. SprA2 expresses PepA2, a toxic peptide which internally triggers bacterial death. Conversely, although PepA2 does not affect bacteria when it is present in the extracellular medium, it is highly toxic to other host cells such as polymorphonuclear neutrophils and erythrocytes. Finally, we showed that SprA2_{AS} expression is lowered during osmotic shock and stringent response, which indicates that the system responds to specific triggers. Therefore, the SprA2/SprA2_{AS} module is not redundant with SprA1/SprA1_{AS}, and its PepA2 peptide exhibits an original dual mode of action against bacteria and host cells. This suggests an altruistic behavior for *S. aureus* in which clones producing PepA2 *in vivo* shall die as they induce cytotoxicity, thereby promoting the success of the community.

INTRODUCTION

Staphylococcus aureus is a serious human bacterial pathogen that causes life-threatening nosocomial and community-acquired infections (1). The success of a staphylococcal infection relies on the coordinated expression of a large set of genes involved in virulence, including toxins and surface proteins (2). Gene expression and the adjustment of bacterial physiology to external signals are both usually dependent on regulators such as regulatory RNAs (sRNAs, also called non-coding RNAs) or transcription factors (2,3). In *S. aureus*, sRNAs range in size from 50 to 500 nucleotides (nt), are usually non-coding, and control the expression of RNA targets that are involved in a wide range of biological processes which include virulence, antibiotic resistance, and central metabolism regulation (4–6). Recently, the sRNA repertoire was compiled into the Staphylococcal regulatory RNA database (SRD: <http://srd.genouest.org/>), which proposes a simple sRNA gene identifier (srn) for each molecule, and acts as a storehouse of useful information for the sRNA community (7). Most *S. aureus* sRNAs act by base-pairing with an RNA target to modulate translation initiation and/or RNA stability. They normally fall into two categories: *cis*- or *trans*-encoded sRNAs (4). *cis*-encoded sRNAs are transcribed from the opposite strand of another RNA (i.e. mRNA or sRNA), and they display perfect sequence complementarity with their target sequences. *trans*-encoded sRNAs are transcribed apart from their targets, and display only partial complementarity with them. Among the *cis*-encoded sRNAs, some studies evidenced the presence of small sense–antisense clusters, some of which can belong to toxin–antitoxin (TA) modules (7–13).

TA modules are divided into six types, and are widespread in bacteria and archaea (14,15). They

*To whom correspondence should be addressed. Tel: +33 223234851; Email: bfelden@univ-rennes1.fr
Correspondence may also be addressed to Astrid Rouillon. Tel: +33 223234394; Email: astrid.rouillon@univ-rennes1.fr

†The authors wish it to be known that, in their opinion, the first two authors should be regarded as Joint First Authors.

Present address: Emilie Camberlein, Université de Nantes, UMR 6286 Unité de Fonctionnalité et Ingénierie des Protéines, 44322 Nantes Cedex 03 France.

share a common feature, which is that they all encode a stable toxin and a labile antitoxin which neutralizes its toxicity (15,16). To date, three types of TA systems (types I, II and III) have been identified in *S. aureus*, and their functions are slowly being elucidated (15,17–20). Among the *S. aureus* TA systems, two belong to type I TA modules and are expressed from pathogenicity islands, genomic islands acquired through horizontal gene transfer. These are SprA1/SprA1_{AS} and SprG1/SprF1 (17,18,20), referred to respectively in the SRD as Srn_3580_SprA1/Srn_3590_SprAs1 and Srn_3840_SprG1/Srn_3830_SprF1 (15). Type I TA modules are composed of a toxic peptide and an unstable antisense sRNA that inhibits toxin translation (21). These peptide toxins have multiple roles. These include small membrane damaging peptides inducing cell death, plasmid maintenance through post-segregational killing, global translation inhibition and commitment to persistence (15,19,21–24). Previous work in our lab revealed that in the Srn_3580_SprA1/Srn_3590_SprAs1 TA pair, Srn_3580_SprA1 expresses a single toxic peptide repressed, in *trans*, by a *cis*-encoded Srn_3590_SprA1_{AS} RNA antitoxin (18). The expression of Srn_3590_SprA1_{AS} sRNA prevents translation initiation of the toxin, allowing the bacterium to grow. More recently, the Srn_3830_SprF1/Srn_3840_SprG1 system was also characterized (20). This module produces two toxic peptides from the same Srn_3840_SprG1 transcript, each causing cell death. Toxicity is counterbalanced in *cis* by the Srn_3830_SprF1 antitoxin, which has dual functions because it represses toxicity at both the transcriptional and translational levels (16). Computational analysis revealed the presence of additional putative TA modules in *S. aureus* which share nucleotide and genetic organization similarities with either Srn_3580_SprA1/Srn_3590_SprAs1 or Srn_3840_SprG1/Srn_3830_SprF1 (13,17,20), and these have been reported in the SRD (7). Here, we describe the functional identification of a novel type I TA system Srn_4540_SprA2_{AS}/Srn_4550_SprA2, which shares 75% sequence similarity with the SprA1/SprA1_{AS} TA system. We provide evidence that the Srn_4540_SprA2_{AS} antisense RNA binds Srn_4550_SprA2 at the ribosomal binding site through partial complementary base-pairing to prevent translation initiation. Based on mutational analysis and cell viability experiments, we demonstrate that SprA2 encodes PepA2, a cytotoxic peptide that also intracellularly triggers *S. aureus* death. We show here that there is no cross-regulation between the SprA2/SprA2_{AS} and SprA1/SprA1_{AS} TA modules, thus demonstrating their specificity. Finally, we also reveal that antitoxin expression is reduced during an osmotic stress and in a stringent medium. These events might be the signals that trigger PepA2 expression to influence colonization, spread and/or infection.

MATERIALS AND METHODS

Bacterial strains, growth, toxin induction, viability assays, and stress conditions

The bacterial strains and plasmids used in this study are listed in Table 1. Except where stated otherwise, cells were

grown in brain heart infusion broth (BHI, Oxoid) or in tryptic soy broth (TSB, Oxoid) under agitation at 37°C. For all experiments, overnight cultures were diluted to an OD_{600 nm} of 0.1, and then monitored at different time points. For co-culture assays, species were mixed to a ratio of 50:50 to reach an OD_{600 nm} of 0.05. When necessary, 5 µg/ml chloramphenicol and/or erythromycin was used, while kanamycin was used at 50 µg/ml. Toxin production was induced by the addition of either 100 nM or 1 µM anhydrotetracycline (aTc). Viability assays were conducted prior aTc induction and then 2.5 h afterwards. For these assays, cell density was adjusted to an OD_{600 nm} of 0.02, 10-fold serial dilutions were performed with BHI, then 10 µl of each dilution was placed on BHI agar plates supplemented with the appropriate antibiotics. For the analysis of RNA levels while undergoing different stresses, *S. aureus* was cultured as previously described (9). Stresses were respectively induced by the addition of 10 mM H₂O₂ (for oxidative stress), HCl (to lower the pH to 5.5), or NaOH (to increase the pH to 9.5), or by changing the temperature to 18 or 42°C (cold and heat shocks). In addition, 60 ml of culture was centrifuged at 4500 rpm for 8 min at room temperature, and the pellets resuspended in TSB supplemented with 1 M NaCl (osmotic stress); in NZM medium (stringent response); or in fresh TSB as a control.

Total RNA extractions

Cells were harvested by centrifugation at 4500 rpm for 10 min at 4°C, and pellets washed with 500 µl lysis buffer (20 mM sodium acetate, 1 mM EDTA, 0.5% SDS, pH 5.5). Cell pellets were broken using acid-washed glass beads (Sigma) in the presence of phenol (pH 4) in a FastPrep FP120 cell disrupter (MP Biomedicals) for 30 s at a power setting of 6.5. Lysates were centrifuged at 16 000 g for 10 min at 4°C. Total RNAs were extracted with phenol/chloroform and precipitated overnight at –20°C with ethanol supplemented with 0.3 M sodium acetate.

Northern blot analysis, RNA stability assays and RACE mapping

Northern blots were performed as previously described (9). Briefly, 10 µg of total RNAs were loaded and separated in 8% polyacrylamide/8M urea gels. The RNAs were probed with ^γ32P 5'-end labeled oligonucleotides (Supplementary Table S1) and detected using a Typhoon FLA 9500 scanner (GE Healthcare). RNA half-life determinations were done using 200 µg/ml rifampicin, with or without 100 nM aTc. *Staphylococcus aureus* Newman strain with pALC_sprA2 + pCN35_sprA2_{AS} was cultured for 2 h, and SprA2 induced by the addition of aTc. After 30 min induction, rifampicin was added to the culture and total RNAs extracted at different time intervals. RNA amounts were quantified using a Typhoon FLA 9500 scanner (GE Healthcare) and tmRNA as an internal loading control. RACE mapping (rapid amplification of cDNA ends) was performed as previously described (20) using the primers listed in Supplementary Table S1.

Table 1. Bacterial strains and plasmids used in this study

Strains and plasmids	Characteristics	References
<i>S. aureus</i> strains		
Newman	Methicillin-sensitive <i>S. aureus</i> strain	(58)
$\Delta sprA2 \Delta sprA2_{AS}$	Newman strain deleted for <i>sprA2</i> and <i>sprA2_{AS}</i> and containing <i>Km^R</i> cassette	This study
N315	Erythromycin-resistant <i>S. aureus</i> strain	(59)
Other strains		
XL-1 Blue	<i>recA1 endA1 gyrA96 thi-1 hsdR17 supE44 relA1 lac</i> [F'proAB lacF ⁺ Z Δ M15Tn10 (Tet ^r)]	Stratagene
EC101	Kanamycin-resistant <i>Escherichia coli</i> strain	(60)
<i>Salmonella typhimurium</i>	<i>Salmonella enterica</i> serovar Typhimurium LT2	(61)
<i>E. faecium</i> Aus004	<i>Enterococcus faecium</i> strain Aus004	(62)
Plasmids		
pALC	pALC2073 with the tetracycline-inducible <i>Pxyl/tetO</i> promoter with <i>Amp^R</i> in <i>E. coli</i> and <i>Chlo^R</i>	(63)
pALC_ <i>sprA1</i>	pALC2073 with <i>sprA1</i> cloned under <i>Pxyl/tetO</i> promoter	This study
pALC_ <i>sprA2</i>	pALC2073 with <i>sprA2</i> cloned under <i>Pxyl/tetO</i> promoter	This study
pALC_ <i>sprA2^{AS3T.T54A}</i>	pALC2073 with <i>sprA2^{AS3T.T54A}</i> cloned under <i>Pxyl/tetO</i> promoter	This study
pALC_ <i>sprA2^{G52C}</i>	pALC2073 with <i>sprA2^{G52C}</i> cloned under <i>Pxyl/tetO</i> promoter	This study
pCN35c	Modified high-copy-number shuttle with <i>Amp^R</i> in <i>E. coli</i> and <i>Chlo^R</i> instead of <i>Erm^R</i> in <i>S. aureus</i>	(29)
pCN35c_ <i>sprA2</i> Flag	pCN35c with <i>sprA2</i> under its own promoter and fused with <i>flag</i> at the 5' end	This study
pCN35c_ <i>sprA2</i> Flags_ <i>sprA2_{AS}</i>	pCN35c_ <i>sprA2</i> Flag containing <i>sprA2_{AS}</i> under its own promoter	This study
pCN35c_ <i>sprA1_{AS}</i>	pCN35c with <i>sprA1_{AS}</i> under its own promoter	This study
pCN35c_ <i>sprA2_{AS}</i>	pCN35c with <i>sprA2_{AS}</i> under its own promoter	This study
pCN41	Vector carrying <i>blaZ</i> , reporter gene and conferring <i>Amp^R</i> in <i>E. coli</i> and <i>Erm^R</i> in <i>S. aureus</i>	(29)
pCN41_ <i>PsprA2_{AS}</i>	pCN41c with <i>blaZ</i> under the control of <i>PsprA2_{AS}</i>	This study
pCN35	High-copy-number shuttle with <i>Amp^R</i> in <i>E. coli</i> and <i>Erm^R</i> in <i>S. aureus</i>	(29)
pCN35_ <i>sprA1_{AS}</i>	pCN35 with <i>sprA1_{AS}</i> under its own promoter	This study
pCN35_ <i>sprA2_{AS}</i>	pCN35 with <i>sprA2_{AS}</i> under its own promoter	This study

Western blots

Recombinant plasmids (Table 1) were transformed in *S. aureus* as previously described (25). *S. aureus* was cultured in BHI broth supplemented with the appropriate antibiotics at 37°C and under agitation until reaching an appropriate OD_{600nm} (see Results). Cells were harvested by centrifugation, and cellular protein extracts were prepared with protease inhibitors as previously described (9). Proteins from the supernatants were precipitated with trichloroacetic acid (TCA), then washed with acetone as previously described (9). Samples were separated on 16% Tricine-SDS-PAGE gels and transferred onto Hybond P PVDF membranes (Amersham). After overnight blocking at 4°C under gentle agitation, the membranes were incubated with horseradish peroxidase-conjugated (HRP) anti-FLAG antibodies (Sigma). The membranes were revealed using an ECL Prime western blotting detection kit (Amersham) and scanned with an ImageQuant LAS 4000 (GE).

Peptide synthesis, hemolytic and cytotoxic assays

PepA2 and PepA1 peptides were synthesized by automated solid-phase synthesis with the kind help of Dr Baudy-Floc'h's CORInt group (ISCR-UMR 6226, University of Rennes 1), and characterized as described previously (26). High-performance liquid chromatography (HPLC) analysis was done to ensure that the purity of the final products was above 95%, and their expected molar mass was confirmed by matrix-assisted laser desorption/ionization time-of-flight mass spectrometry (MALDI-TOF).

Cytotoxic assays were conducted using human blood provided by the Etablissement Français du Sang from at least three independent samples (EFS Rennes). For hemolytic assays, blood was washed and then resuspended

at 5% (v/v) in phosphate-buffered saline (PBS). The peptide solutions were added at 2× concentrations to V-bottom 96-well plates after which 75 µl of 5% blood was added. The negative control was performed using PBS instead of peptides, while 100% hemolysis was assessed using 1% Triton X-100. Plates were incubated for 2 h at 37°C, then centrifuged at 1400 rpm for 15 min at room temperature. Finally, 100 µl supernatant was transferred into a flat-bottom 96-well plate and the OD_{414 nm} measured to assess the presence of released haemoglobin.

Polymorphonuclear neutrophils (PMNs) were isolated using the EasySep™ Direct Human Neutrophil Isolation kit (Stemcell) per the manufacturer's recommendations. Neutrophils were resuspended in RPMI medium supplemented with 2% fetal veal serum (FVS), then 20 000 neutrophils were distributed in each of the 96 wells of a tissue culture plate. Cells were incubated for 2 h at 37°C and 5% CO₂ with increasing concentrations of PepA2. Neutrophils were harvested by centrifugation at 350 g for 8 min at 4°C, washed with RPMI 2% FVS, then stained with 50 µg/ml propidium iodide (PI) (Sigma-Aldrich) for 15 min in the dark at room temperature. After washing, cell viability was determined and analysed on a BD Biosciences LSR II cytometer using FACSDiva™ software. Since PI is not permeant to live cells, the percentage of unstained PMNs corresponds to the viable cell count.

In vitro transcription and translation assays

In vitro transcription was conducted from PCR-amplified fragments cloned into pUC19 under the control of the T7 promoter, and containing a HaeIII restriction site at the sequence's 3' end. Plasmids were linearized with HaeIII and subjected to *in vitro* transcription using the MEGAscript T7 kit (Thermo Fisher) according to the manufacturer's rec-

ommendations. RNAs were gel-purified, eluted, and precipitated with ethanol in the presence of 0.3 M sodium acetate. The *in vitro* translation assay was performed with [³⁵S]-methionine using an *E. coli* S30 extract system for linear templates (Promega) as per the manufacturer's instructions.

Electrophoretic mobility shift assays and toeprints

RNAs were probed with oligonucleotides labelled at the 5' ends with ^γ32P. For electrophoretic mobility shift assays, RNAs were denatured in buffer (80 mM HEPES pH 7.5, 330 mM KCl, 4 mM MgCl₂) for 2 min at 80°C, chilled on ice, then refolded for 20 min at 20°C. Binding was conducted in 10 μl for 30 min at 30°C. 0.1 pmol of labelled RNA was incubated with increasing amounts of unlabeled RNA. The specificity of the complex was assessed by adding an excess of unlabeled RNA (for concentrations used, see Figures 6 and 8). Samples were supplemented with glycerol to a final concentration of 10%, then loaded onto native 8% polyacrylamide gels containing 5% glycerol. Electrophoresis was performed in 0.5× Tris–borate–EDTA buffer at 4°C and 100 V. The results were analysed on a PhosphorImager and *K_d* values determined accordingly.

For toeprinting assays, annealing mixtures containing 0.25 pmol unlabelled SprA2 and 1.5 pmol labelled primer in a buffer (20 mM Tris-acetate pH 7.5, 60 mM NH₄Cl, 1 mM DTT) were incubated for 1 min at 90°C, and then quickly chilled on ice for 1 min. Renaturation was done in 10 mM MgCl₂ at 20°C for 15 min. The influence of SprA2_{AS} was assayed by adding 0.25 pmol to the annealing mixtures, then incubating for 5 min at 37°C. Purified *Escherichia coli* 70S ribosomes were diluted in the reaction buffer in the presence of 1 mM MgCl₂ then activated for 15 min at 37°C. For each sample, 4 pmol purified 70S ribosomes were added, followed by 5 min incubation at 37°C and adjustment of the MgCl₂ concentration to 10 mM. After 10 min at 37°C, 10 pmol tRNA^{Met} was added and the samples were incubated for 5 min at 37°C. The cDNAs were synthesized using 4 units AMV RT (New England Biolabs) for 15 min at 43°C. The reaction was stopped by adding 10 μl loading buffer II (Ambion). The samples were incubated for 5 min at 95°C, then placed on ice. The cDNAs were loaded and separated onto 8% urea–PAGE gels. The toeprint position on SprA2 was determined by DNA sequencing, and the results were analysed on a PhosphorImager.

Reporter gene experiments

Overnight cultures were adjusted to an OD_{600 nm} of 0.1. For each time point, cells were centrifuged and resuspended in 1× PBS to obtain an equal cell density throughout the assay. Cell lysis was performed using 0.7 mg/ml lysostaphin, 0.2 U/μl benzonase and 0.1 mM MgCl₂ at 37°C for 20 min. After adding 0.25 mg/ml nitrocefin (a β-lactamase substrate), β-lactamase activity was quantified on a BioTek instrument every 10 min for 40 min at 492 nm. This activity was normalized against the protein quantities determined by a Bradford assay.

RESULTS

Both *sprA2* and *sprA2_{AS}* genes are expressed in *Staphylococcus aureus*

The *S. aureus* Newman *srn_4540_sprA2_{AS}/srn_4550_sprA2* locus was identified based on its 75% sequence similarity with the pair *srn_3580_sprA1/srn_3590_sprA1_{AS}* (7,13,17) (Supplementary Figure S1). For simplicity, they are referred to here as SprA1, SprA2, SprA1_{AS} and SprA2_{AS}. As shown in Figure 1A, the *sprA2/sprA2_{AS}* pair is located in the core genome of *S. aureus* Newman, between genes encoding a hypothetical protein and one in the GtrA family. To demonstrate and study their expression during bacterial growth, we designed novel probes (Figure 1B). Growth conducted in BHI (upper chart) showed that both *srna* genes were transcribed and detected by northern blots. While the SprA2 levels were similar to those of the tmRNA control, the intensity of the SprA2_{AS} bands varied in a different manner than the control. We quantified each band to determine the relative SprA2_{AS} RNA levels. These increased by around 1.8-fold after 4 h growth, which corresponds to the post-exponential phase, which indicates that there were therefore only moderate SprA2_{AS} variations under these conditions. We then did RACE mapping to determine the 5' and 3' boundaries, confirming that both genes overlap in their 3' regions (see Figure 1A for the coordinates resulting from RACE). We used IntaRNA software (27) for *in silico* exploration of the two RNA sequences. This showed that, as for the *sprA1/sprA1_{AS}* pair, these two RNAs could interact *in trans* with their 5' regions through partial pairings (Figure 1C), with SprA2_{AS} binding SprA2 both at a putative ribosomal binding site and at its adjacent start codon, suggesting that it could indeed act as a type I TA system.

SprA2/SprA2_{AS} is a functional type I toxin–antitoxin system that triggers *Staphylococcus aureus* cell death

We further investigated the *sprA2/sprA2_{AS}* module to verify whether it encodes a functional type I TA system. To that aim, we cloned *sprA2* into pALC (28), allowing anhydrotetracycline-inducible expression, and cloned *sprA2_{AS}* into high-copy-number pCN35 under its own promoter (29). We induced SprA2 expression by adding 1 μM aTc, then monitored *S. aureus* growth for 8 h (Figure 2A). While cells replicating both empty vectors exhibited typical bacterial growth (squares), growth of the *S. aureus* cells overexpressing only SprA2 was immediately arrested, with OD measurements decreasing by ~50% over the next 6 h, suggesting cell death (circles). To some extent, this sudden arrest was relieved by the concomitant episomal expression of SprA2_{AS} (triangles). In this case, bacterial growth resumed after an apparent stasis of 2 h, finishing with a biomass close to that of the control strain. To further confirm that the decreased OD observed with SprA2 overexpression was due to bacterial death, serial dilutions of the respective cultures were plated without aTc (Figure 2B). Prior to induction, not much difference was observed between the three clones (left panel). However, most cells that overexpressed SprA2 did not grow on agar plates, indicating that they were not viable (right panel). Cell death was counterbalanced when SprA2_{AS} was overexpressed in pCN35,

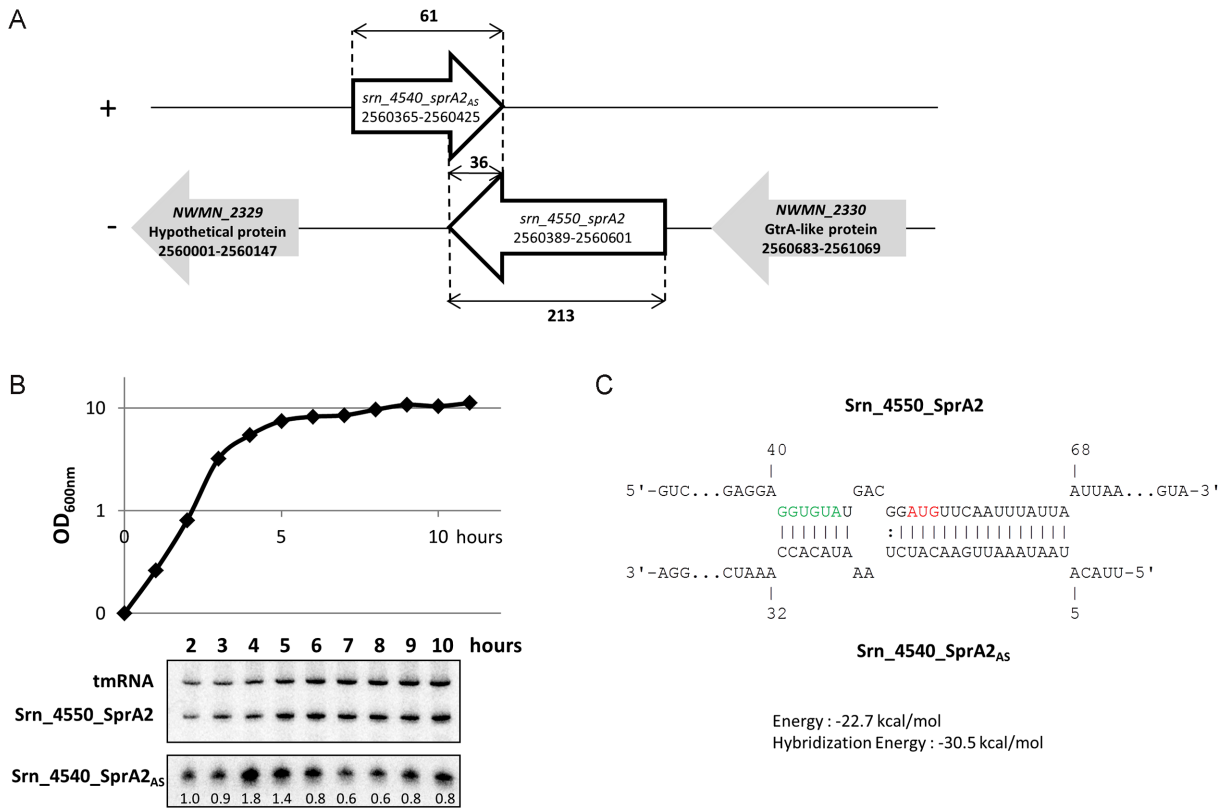


Figure 1. The putative type I toxin–antitoxin module *Srn_4550_sprA2/Srn_4540_sprA2_{AS}* is expressed in *Staphylococcus aureus* Newman. (A) Schematic of the genetic organization of the *srn_4550_sprA2/srn_4540_sprA2_{AS}* locus. (B) *Srn_4550_sprA2/Srn_4540_sprA2_{AS}* expression profile during growth in BHI. Growth was monitored by measuring the optical density at 600 nm (OD_{600nm}) every hour (upper chart). Expression was monitored by northern blotting, with tmRNA as an internal loading control (lower chart), with the relative amount of *Srn_4540_SprA2_{AS}* RNA indicated under each band. (C) *In silico* best prediction of the molecular interaction between the two components made with intaRNA program. The putative ribosome-binding site is green and the start codon is red. The coordinates appearing on panels A and C were experimentally determined by RACE mapping.

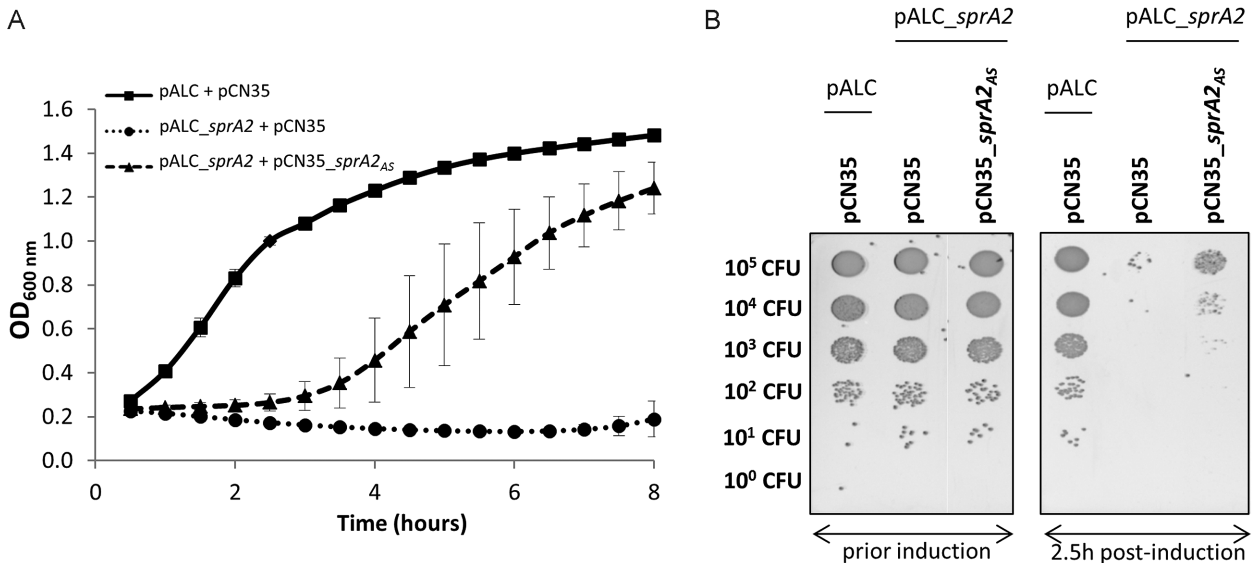


Figure 2. *sprA2/sprA2_{AS}* encodes and expresses a functional toxin–antitoxin system. (A) Comparative growth curves after induction with 1 μM anhydrotetracycline (aTc) on *Staphylococcus aureus* Newman replicating empty plasmids pALC and pCN35 (squares); pALC_{sprA2} and pCN35 (circles); and pALC_{sprA2} and pCN35_{sprA2_{AS}} (triangles). Growth was conducted in a Biotek instrument for 2.5 h, then expression was induced by aTc. Data points shown represent the growth after this addition, and are the mean of three independent biological replicates. (B) Assessment of cell viability by plating 10-fold serial dilutions, prior induction (left panel) or 2.5 h post-induction (right panel). All cultures (broth and agar) contain chloramphenicol and erythromycin concentrations appropriate for plasmid maintenance.

although complete suppression of toxicity could not be achieved. Similar experiments were performed with the *sprA1/sprA1_{AS}* system (Supplementary Figure S2), known to have antibacterial activity. Here, *SprA1* overexpression led to cell death which was fully relieved by *SprA1_{AS}* overexpression, suggesting that *SprA2* RNA expression leads to stronger toxicity than does *SprA1*. To verify whether cell toxicity was due to the expression of a peptide rather than the *SprA2* RNA itself, we tagged *PepA2* with a FLAG sequence at its N-terminus. As described previously, the addition of a FLAG sequence usually decreases peptide toxicity, allowing for its expression to be monitored (17). Then, to avoid any potential repression of ^{FLAG}*PepA2* expression by endogenous *SprA2_{AS}*, we deleted the entire putative type I TA locus in the Newman strain. We expressed *SprA2-FLAG* under its own promoter and in the presence or absence of *SprA2_{AS}* in Newman Δ *sprA2* Δ *sprA2_{AS}* (Figure 3A and Supplementary Figure S3). Western blotting indicated that a peptide was expressed from *sprA2*, especially at OD_{600 nm} values of 1 and 2, and that the presence of *SprA2_{AS}* lowered peptide expression. Additionally, we collected the growth supernatant and found that a fraction of the ^{FLAG}*PepA2* was released in the extracellular medium, mostly at OD_{600 nm} of 6 and in the absence of *SprA2_{AS}* (Figure 3A). To prevent *PepA2* expression, we made point mutations in *sprA2*, as shown in Figure 3B. Each mutated version was cloned into pALC and expression was induced with a Tc (Figure 3C). Mutating the start codon (*SprA2*^{A53T,T54A}) to prevent translation initiation did not inhibit growth. Since this absence of growth inhibition could be due to a substantial structural modification in *SprA2* RNA rather than to a lack of *PepA2* expression, we generated a point mutation just before the start codon that allows translation (*SprA2*^{G52C} in Figure 3B). This construct led to a sudden growth arrest similar to that observed previously, confirming that toxicity is dependent on *PepA2* expression and that it is not due to the RNA. Altogether, our results indicate that *sprA2/sprA2_{AS}* encodes a functional type I TA system, with *sprA2* triggering *S. aureus* death.

PepA2 kills *Staphylococcus aureus* intracellularly and acts as an extracellular cytotoxin against human erythrocytes and polymorphonuclear neutrophils

We pursued our investigations on cell toxicity, conducting co-cultures with both Gram-positive and Gram-negative bacteria. The bacteria were mixed at equal optical densities, and growth was followed in a Biotek instrument. After 2.5 h growth, cultures were subjected to 1 μ M aTc to promote *SprA2* expression (Figure 4). For all co-cultures tested, we could discriminate the species based on the use of selective or elective media (Supplementary Figure S4). When mixed with erythromycin-resistant *S. aureus* N315, *S. aureus* Newman growth stopped upon *SprA2* induction, but N315 continued growing, which indicates that the *SprA2* toxin acts intracellularly and cannot kill *S. aureus* from the outside (Figure 4A and Supplementary Figure S4). Conversely, no significant growth differences were observed in cultures not challenged with aTc (Supplementary Figure S5). We next tested the effects of the toxin on the growth of kanamycin-resistant *Escherichia coli* EC101 (Figure 4B), *Salmonella ty-*

phimurium (Figure 4C), and *Enterococcus faecium* Aus004 (Figure 4D). In all of the tests, *PepA2* overexpression arrested the growth of *S. aureus* Newman pALC-*sprA2*, but not of the other species. To confirm that extracellular *PepA2* was inefficient for bacterial killing, we chemically synthesized and purified *PepA2*. Synthetic *PepA2* was added to bacterial cultures at various concentrations to determine the minimum inhibitory concentration (MIC). *PepA2* did not substantially inhibit the growths of *S. aureus*, *E. coli* or *S. typhimurium*, and only weakly inhibited *E. faecium* (Supplementary Figure S6). Furthermore, *SprA2* overexpression in *E. coli* inhibited growth, indicating that *PepA2* can also target Gram-negative bacteria from the inside, although not from the outside (Supplementary Figure S7). We further characterized synthetic *PepA2*'s toxic activity by adding it extracellularly to human erythrocytes and to polymorphonuclear neutrophils (PMNs) from different blood donors (Figure 5). *PepA2* was highly hemolytic, with 50% hemolysis (H₅₀) reached with \sim 0.4 μ M *PepA2* (Figure 5A). On the other hand, chemical synthesis of *PepA1* and its subsequent use for hemolysis revealed that more than 30 μ M of this peptide was needed to obtain the same effect on human red blood cells (Figure 5B). We next tested the cytotoxic effect of *PepA2* against PMNs (Figure 5C). *PepA2* was also cytotoxic in this case, with an IC₅₀ around 6 μ M. Taken together, our data indicate that *PepA2* induces bacterial cell death internally and, when it is released in the medium it is cytotoxic against human host cells, but not efficiently antibacterial.

The non-overlapping 5' end of *SprA2_{AS}* regulates toxin production and prevents *PepA2* translation initiation

To investigate the regulation between the toxin and anti-toxin RNA in the *sprA2/sprA2_{AS}* type I TA system, we began with gel shift assays. We mixed labelled *SprA2* with increasing amounts of *SprA2_{AS}* and found that the RNAs interact to form a complex (Figure 6A). This indicated a direct RNA-RNA interaction, without the need of a third party. The apparent binding constant between the two is \sim 13 nM, and the complex formation specificity was assessed by adding a 50-fold excess of various unlabelled RNAs (Figure 6A, last three lanes). While an excess of unlabelled *SprA2* displaced the complex, the addition of unrelated *Srn.3610.SprC* sRNA (30) or a fragment of autolysin mRNA did not modify the binding of *SprA2_{AS}* onto *SprA2* RNA, implying specificity. We then went on to examine whether the 5' non-overlapping region of *SprA2_{AS}* was responsible for the interaction between the two RNAs (Figure 6B and C). For this, we transcribed 5' and 3' moieties of *SprA2* and *SprA2_{AS}* (Supplementary Figure S8). As shown in Figure 6B, only the 5' half of *SprA2_{AS}* formed a specific complex with *SprA2*. Similarly, unlabelled *SprA2_{AS}* only slowed the migration of 5' *SprA2* (Figure 6C). These results indicate that the 5' non-overlapping domains of both RNAs interact together *in vitro*, and demonstrate that although they are transcribed from the same locus (Figure 1A and C), *SprA2_{AS}* regulates *SprA2* expression *in trans*.

As presented in Figure 1C, this *trans*-regulation is predicted to mask the *SprA2* ribosomal binding site (RBS). We therefore conducted toeprinting assays to see whether

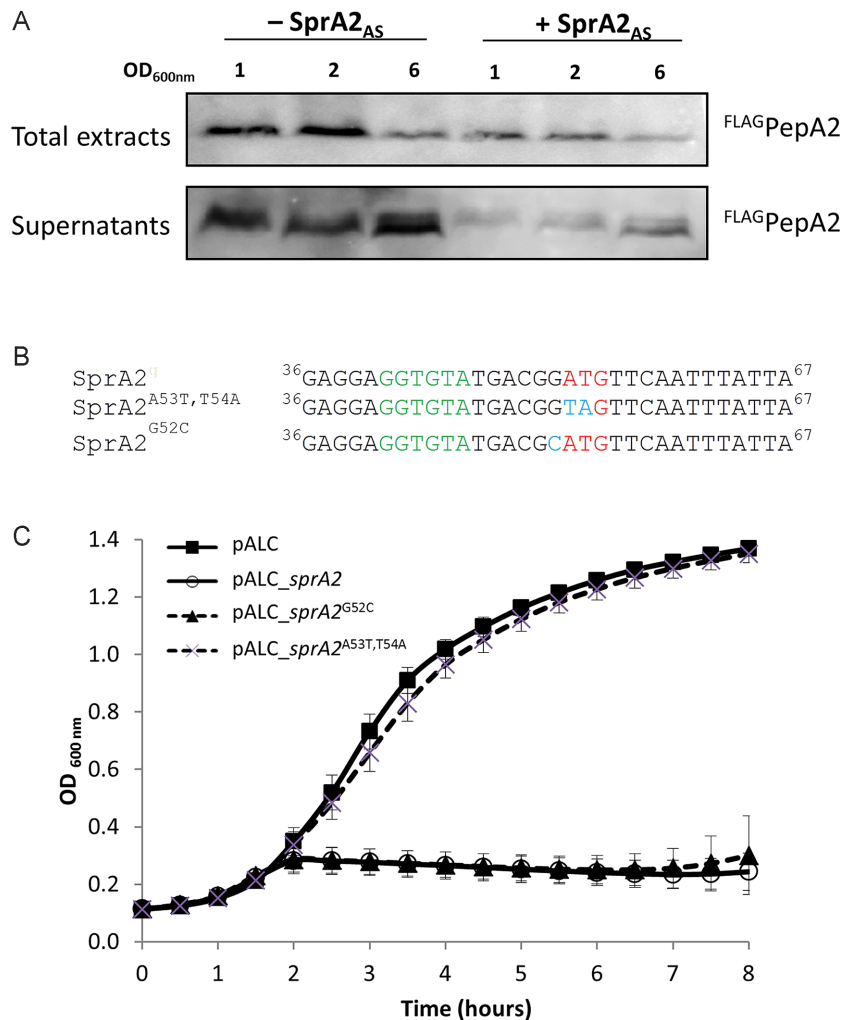


Figure 3. Bacterial toxicity is linked to the expression of PepA2. (A) *In vivo* expression of flagged PepA2, comparing *Staphylococcus aureus* Newman strains $\Delta sprA2 \Delta sprA2_{AS}$ pCN35_ sprA2Flag compared to Newman $\Delta sprA2 \Delta sprA2_{AS}$ pCN35_ sprA2Flag sprA2_{AS}. (B) Point mutations were done in *sprA2* to avoid translation initiation or to modify RNA secondary structure. (C) Comparative growth curves of Newman strain containing empty plasmid pALC (squares); pALC_ sprA2 (circles); pALC_ sprA2^{G52C} (triangles); or pALC_ sprA2^{A53T, T54A} (crosses). Induction was done after 2 h with 1 μ M anhydrotetracycline (aTc).

SprA2_{AS} would compete with ribosome binding onto SprA2. We began by looking at SprA2 in the presence of increasing amounts of purified *E. coli* ribosomes (Figure 7A). The assays showed that SprA2 recruits ribosomes to form translation initiation complexes in the presence of the initiator tRNA^{fMet}. From 1 pmol of 70S ribosomes, the toeprint was detected approximately 14 nucleotides downstream from the predicted initiation codon (Figure 7A, lanes 9 and 10). We then tested whether the antitoxin SprA2_{AS} could prevent ribosomal loading onto SprA2 (Figure 7B), so the antitoxin and/or ribosomes were mixed with SprA2. A strong pause was detected starting at position A72 during the reverse transcription of SprA2 in the presence of its RNA antitoxin (Figure 7B, lane 6), suggesting that the association between the two RNAs induces a structural modification in SprA2 which prevents primer extension. The addition of both SprA2_{AS} and ribosomes resulted in an absence of ribosomal loading, whereas the pause due

to the antitoxin's presence was still detected (Figure 7B, lane 8 and right panel). This indicated that SprA2_{AS} prevents ribosomal loading onto SprA2 and therefore PepA2 translation. To support this, we performed *in vitro* translation of SprA2 in the presence of either the full-length RNA antitoxin or its 5' or 3' truncated versions (Figure 7C). Whereas SprA2 translation did occur *in vitro* (lane 1), it was inhibited by both SprA2_{AS} and by the truncated version containing the main binding domain (lanes 2 and 3). Conversely, the 3' part of the antitoxin did not significantly inhibit translation (lane 4). Also, the addition of non-cognate antitoxin SprA1_{AS} did not prevent translation *in vitro* (lane 5), suggesting that members of the SprA TA systems are specific to each other. SprA2_{AS} thus regulates the expression of SprA2, at least at the translational level, and its non-overlapping 5' domain binds SprA2 at the RBS to prevent ribosomal loading and PepA2 expression.

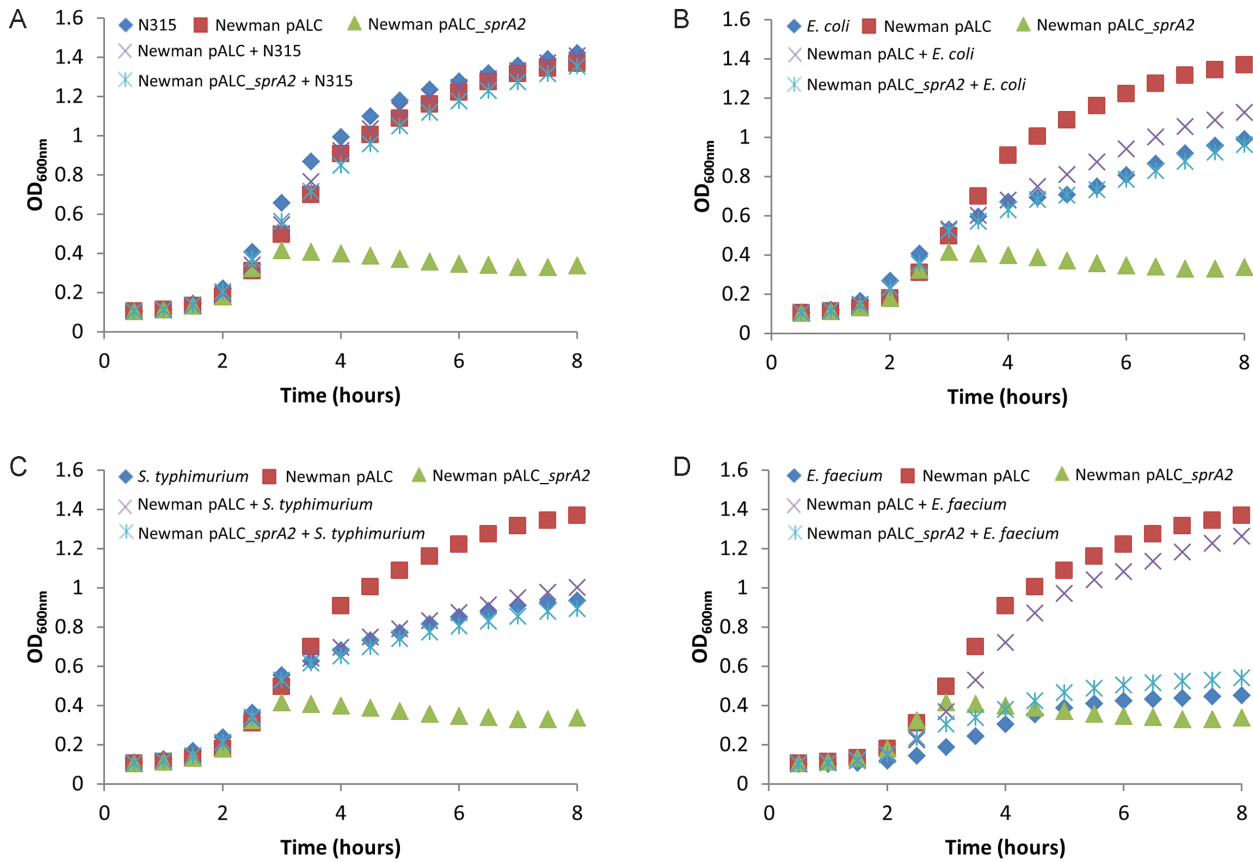


Figure 4. The SprA2 toxin does not kill other bacteria during co-cultures. (A) The effects of *sprA2* expression on the growth of *Staphylococcus aureus* N315. Shown are: *S. aureus* N315 (blue diamonds); *S. aureus* Newman pALC (red squares); Newman pALC_*sprA2* (green triangles); Newman pALC + N315 (purple crosses); and Newman pALC_*sprA2* + N315 (blue crosses). (B) The effects of *sprA2* expression on *Escherichia coli* growth. Shown are: *E. coli* EC101 (blue diamonds); *S. aureus* Newman pALC (red squares); Newman pALC_*sprA2* (green triangles); Newman pALC + *E. coli* (purple crosses); and Newman pALC_*sprA2* + *E. coli* (blue crosses). (C) The effects of SprA2 expression on *Salmonella typhimurium* growth. Shown are: *S. typhimurium* (blue diamonds); *S. aureus* Newman pALC (red squares); Newman pALC_*sprA2* (green triangles); Newman pALC + *S. typhimurium* (purple crosses); and Newman pALC_*sprA2* + *S. typhimurium* (blue crosses). (D) The effects of SprA2 expression on *Enterococcus faecium* growth. Shown are: *E. faecium* Aus004 (blue diamonds); *S. aureus* Newman pALC (red squares); Newman pALC_*sprA2* (green triangles); Newman pALC + *E. faecium* (purple crosses); and Newman pALC_*sprA2* + *E. faecium* (blue crosses). Growth was conducted in a Biotek instrument and 1 μ M aTc was added after 2.5 h. The data presented are the mean of three independent experiments performed in triplicate. To improve readability, the standard deviations (which never exceeded 0.057) were omitted.

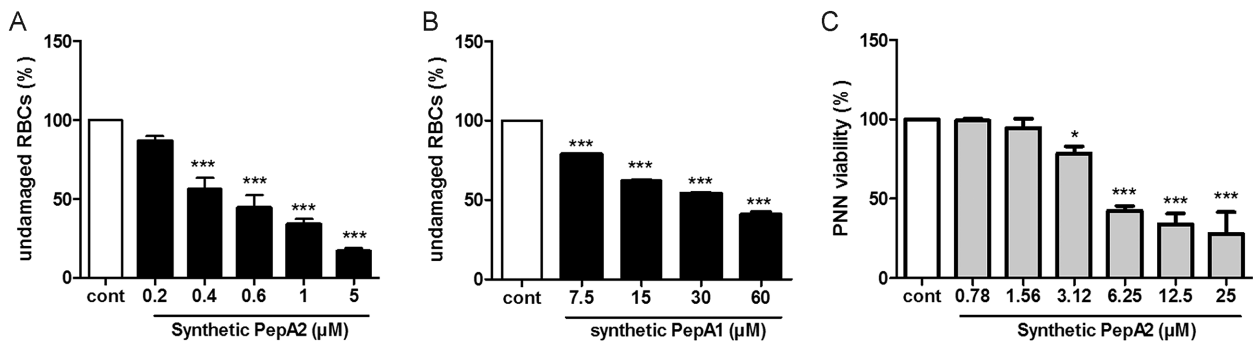


Figure 5. SprA2 is cytotoxic against human erythrocytes and polymorphonuclear neutrophils (PMNs) from blood donors. (A) Hemolytic activity of synthetic SprA2-encoded peptides on human erythrocytes (RBCs). (B) Hemolytic activity of synthetic SprA1-encoded peptides on human RBCs. (C) Cytotoxicity of synthetic SprA2-encoded peptides on PMN was estimated by flow cytometry using propidium iodide staining. The data are the mean of at least three independent biological experiments performed in triplicate. * $P < 0.05$; *** $P < 0.001$.

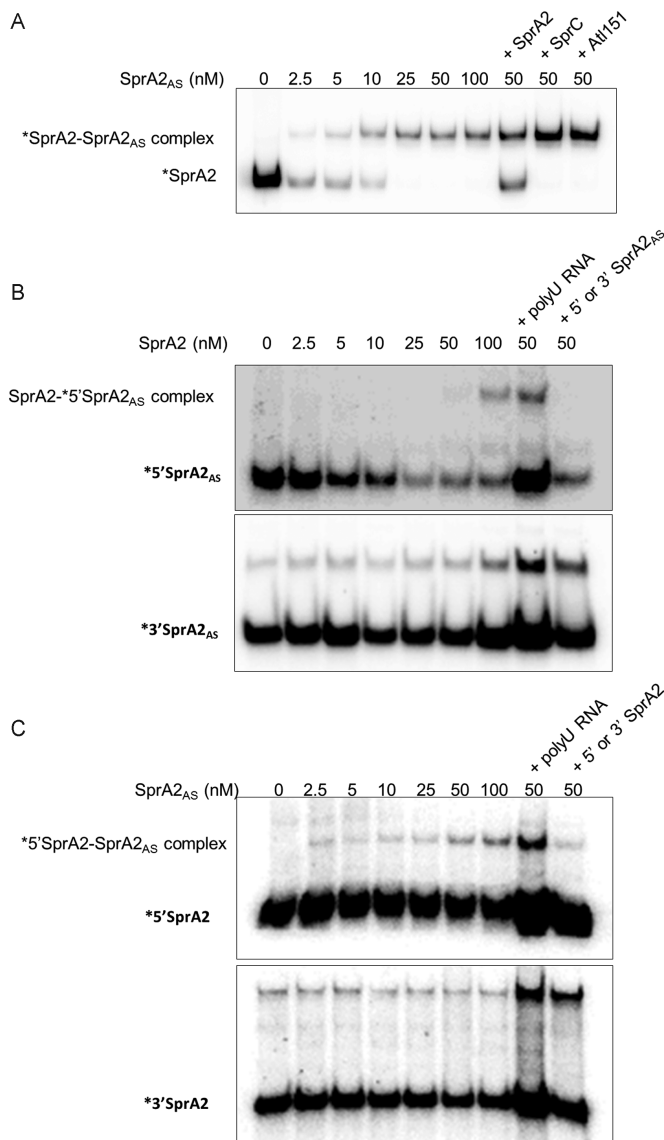


Figure 6. The non-overlapping domains of the SprA2 and SprA2_{AS} RNAs interact with each other. (A) Native gel shift assays of purified labelled SprA2 with increasing amounts of unlabelled SprA2_{AS}. To assess binding specificity, 500 nM unlabelled SprA2, SprC, and Atl were individually added to the complex. (B) Complex formation between 5' or 3' SprA2_{AS} and SprA2. To assess complex formation specificity, 200 nM truncated SprA2_{AS} and 2 μ M polyuridine (polyU) RNAs were added. (C) Complex formation between 5' or 3' SprA2 and SprA2_{AS}. To assess complex specificity, 200 nM truncated SprA2 and 2 μ M of polyU RNAs were added. Labelled RNAs (10 nM in each gel) are indicated with asterisks. The upper bands present in the lower panels of B and C represent unspecific bands as it is also detected in the absence of a potential partner (lanes 1). The data illustrate one representative experiment from three independent replicates.

The SprA2/SprA2_{AS} and SprA1/SprA1_{AS} pairs act independently, with no cross-regulations between the antitoxins to rescue cell toxicity

These results revealed a regulation mechanism similar to that observed in the SprA1/SprA1_{AS} TA system (17). However, although both TA systems have nucleotide sequence similarities (Supplementary Figure S1), *in vitro* translation assays indicated that SprA1_{AS} cannot inhibit SprA2 trans-

lation. Therefore, we wondered whether the TA systems act independently, or if there is a cross-reactivity. First, we performed gel shift assays to demonstrate whether such cross interactions can occur *in vitro* (Figure 8A). When increasing amounts of unlabelled SprA2_{AS} RNA were added to labelled SprA2 or SprA1 RNA, RNA-RNA interactions were observed only between SprA2 and SprA2_{AS} (Figure 8A, left panel). Conversely, unlabelled SprA1_{AS} RNA only slowed the migration of labelled SprA1 (Figure 8A, right panel), indicating that both TA systems are specific to themselves *in vitro*. To support this, we tested the potential of each antitoxin to interact with their non-cognate toxins during bacterial culture. Genes coding the toxins were cloned into the aTc-inducible pALC vector, while the antitoxins were cloned into pCN35 under their own promoters (Figure 8B). Cell death due to SprA2 overexpression was not relieved by the presence of the SprA1_{AS} antitoxin (Figure 8B; crosses in left panel), consistent with the *in vitro* results. Similarly, SprA1 toxicity was relieved only when its SprA1_{AS} cognate antitoxin was expressed from pCN35 (Figure 8B, right panel). Total RNA extractions performed under these growth conditions confirmed that all of the TA module components were expressed, and that overexpression of SprA2 or SprA1 was indeed effective (Figure 8C). While the antitoxin RNA levels did increase when their cognate toxins were induced, the RNA levels of the other antitoxins went down (Figure 8C, conditions 2 to 4). Therefore, we monitored the transcript levels of another type I TA module (SprG1/SprF1) and of two regulatory RNAs, Srn_9340 and Srn_3610_SprC (Supplementary Figure S9). SprF1 and these regulatory RNAs have half-lives of 10, 5 and 20 min, respectively (25,30), and they all showed reduced transcript levels upon SprA1/2 induction. Conversely, the RNA levels of SprG1, which has a half-life of \sim 2 h (20), did not decrease after SprA1/2 induction. This suggests that the decreased levels of RNAs with short or moderate half-lives are probably due to cell death, which favours rapid RNA degradation.

SprA2 overexpression increases the stability of SprA2_{AS} RNA

Increased SprA2_{AS} antitoxin RNA in response to the overexpression of its cognate toxin suggested an effect at the levels of transcription and/or stability. To measure antitoxin expression, we cloned the *sprA2*_{AS} promoter into pCN41, allowing transcriptional fusion with *blaZ*, which encodes β -lactamase. *S. aureus* Newman pCN41-*PsprA2*_{AS} was transformed with either pALC or pALC-SprA2 (Figure 9). A 1.3-fold increase in β -lactamase activity was measured when aTc was added to promote SprA2 expression. Similarly, when aTc was added to the strain co-transformed with pALC, β -lactamase activity increased \sim 1.4-fold, indicating that the inducer itself weakly activates *PsprA2*_{AS} in the absence of SprA2 overexpression. Conversely, no significant variations were detected between strains overexpressing SprA2 and the control, indicating that SprA2 does not directly or indirectly regulate the transcription of its antitoxin. We therefore decided to look at SprA2_{AS} RNA stability with or without SprA2 induction. To do this we used Newman pALC-*sprA2* + pCN35-*sprA2*_{AS} (see Figure

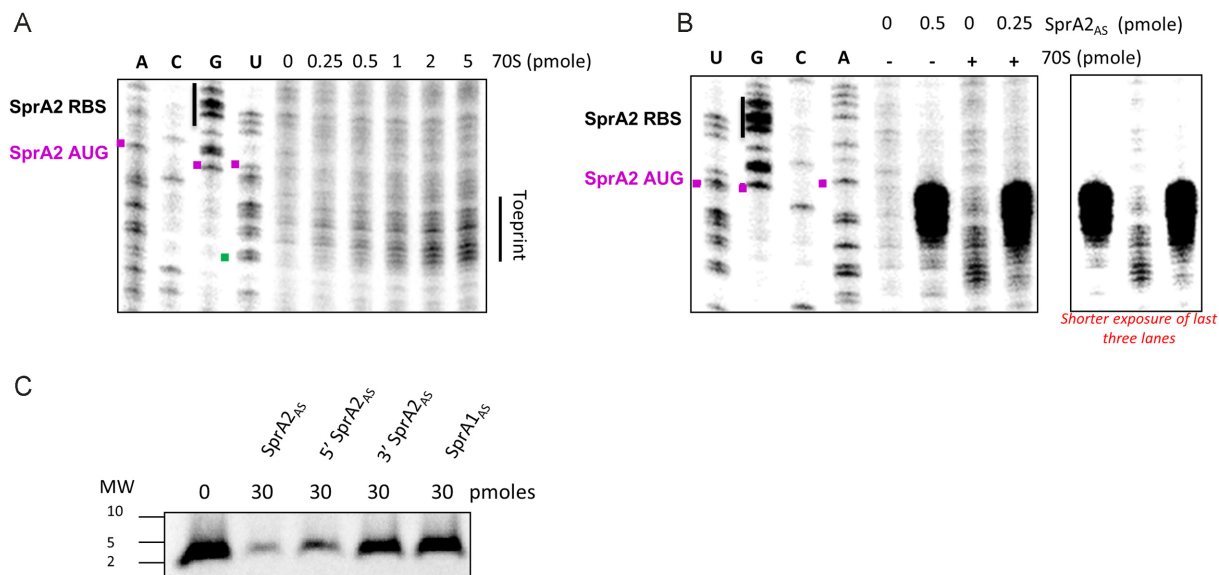


Figure 7. SprA2_{AS} prevents SprA2 translation by using its non-overlapping RNA domain. (A) Toeprinting assays of 0.25 pmol SprA2 in the presence of increasing amounts of purified *E. coli* 70S ribosomes revealed toeprints from position U71. The A, C, G and U lanes represent the SprA2 sequencing lanes. (B) Toeprinting assays of 0.25 pmol SprA2 in the presence of SprA2_{AS} and/or purified *E. coli* 70S ribosomes. The toeprint initially observed from position U71 decreased in the presence of the antitoxin. However, a strong pause appears at position A64 upon SprA2_{AS} addition, suggesting a conformational change in SprA2. In the right panel, a shorter exposure is provided to show the effect of SprA2_{AS} on the toeprint. (C) *In vitro* translation assay of 20 pmol SprA2 in the presence of 30 pmol of SprA2_{AS}, 5' SprA2_{AS} RNA, 3' SprA2_{AS}, or SprA1_{AS} (lanes 1–5, respectively). SprA2 encodes PepA2, a peptide weighing ~4 kDa.

8) and inhibited transcription with rifampicin (Figure 9B). While the half-life of SprA2_{AS} was around 5 min in the presence of endogenous SprA2, SprA2 induction increased its antitoxin's stability by ~9-fold, with a half-life of around 45 min. SprA2 expression thus increases SprA2_{AS} stability, but not its transcriptional activity.

Antitoxin expression levels are reduced under osmotic shock and stringent conditions

The triggers involved in the expression and regulation of this newly described type I TA system are unknown. To explore this question, we applied different stresses, some mimicking the changes encountered by the bacteria during infection. SprA2 and SprA2_{AS} RNA levels were monitored by northern blots after 30 and 60 min stress, then compared with those produced without stress (Figure 10). The Mann-Whitney U test was used to locate statistically significant differences, with biologically relevant differences being anything over the defined cut-off value of 2. The SprA2 RNA levels were weakly affected by all conditions applied (Figure 10A), but although we measured variations, they were always lower than a two-fold change (i.e. a 1.7-fold decrease in 1 M NaCl after undergoing stress for 1 h). Conversely, after 30 or 60 min of stringent (NZM) or osmotic (NaCl) stress, SprA2_{AS} RNA levels significantly decreased (Figure 10B). In 1 M NaCl, antitoxin RNA was decreased more than two-fold, whereas it was lowered by around four in NZM medium. While the RNA levels were affected in these two cases, only a slight decrease (under the cut-off) in SprA2 transcript levels was measured in 1 M NaCl (Figure 10A). Other variations in antitoxin levels were lower than two-fold increases or decreases (Figure 10B). Altogether, these data

indicate that *sprA2* and *sprA2_{AS}* are differentially expressed in response to stressors, with antitoxin RNA levels reduced under stringent conditions and during osmotic shock. In addition, this reduction was not accompanied by a strong change in SprA2 transcript levels. Overall, this suggests that stringent conditions and elevated osmotic pressure could be triggers for promoting PepA2 toxin production.

DISCUSSION

Toxin-antitoxin modules are widespread in bacteria and archaea (14,15). They are known to participate in various functions, including irreversible membrane damage, plasmid maintenance through post-segregational killing, cell death or stasis, global translation inhibition, and a recently discovered role in persistence (15,19,22,24). They are divided into six different types, with three described in *S. aureus* (15). To date, two type-I systems have been characterized in *S. aureus*: the SprA1/SprA1_{AS} and SprG1/SprF1 systems identified and expressed from pathogenicity islands (17,20).

In bacterial genomes, type I TA systems are commonly found in multiple copies. In this work, we describe the SprA2/SprA2_{AS} module, which has more than 70% nucleotide sequence identity with the SprA1/SprA1_{AS} TA system (7,13,17). We report here the second example of a type I TA system in which a *cis*-encoded antitoxin acts in *trans* with its cognate toxin to prevent ribosomal loading and thus the translation of a toxic peptide. We showed that the 5' part of the antitoxin's RNA is sufficient to bind SprA2 RNA *in vitro*, while its 3' moiety, sharing extensive complementary due to the overlapping regions, has only a minor effect on regulation. Indeed, no inhibition of SprA2 translation was

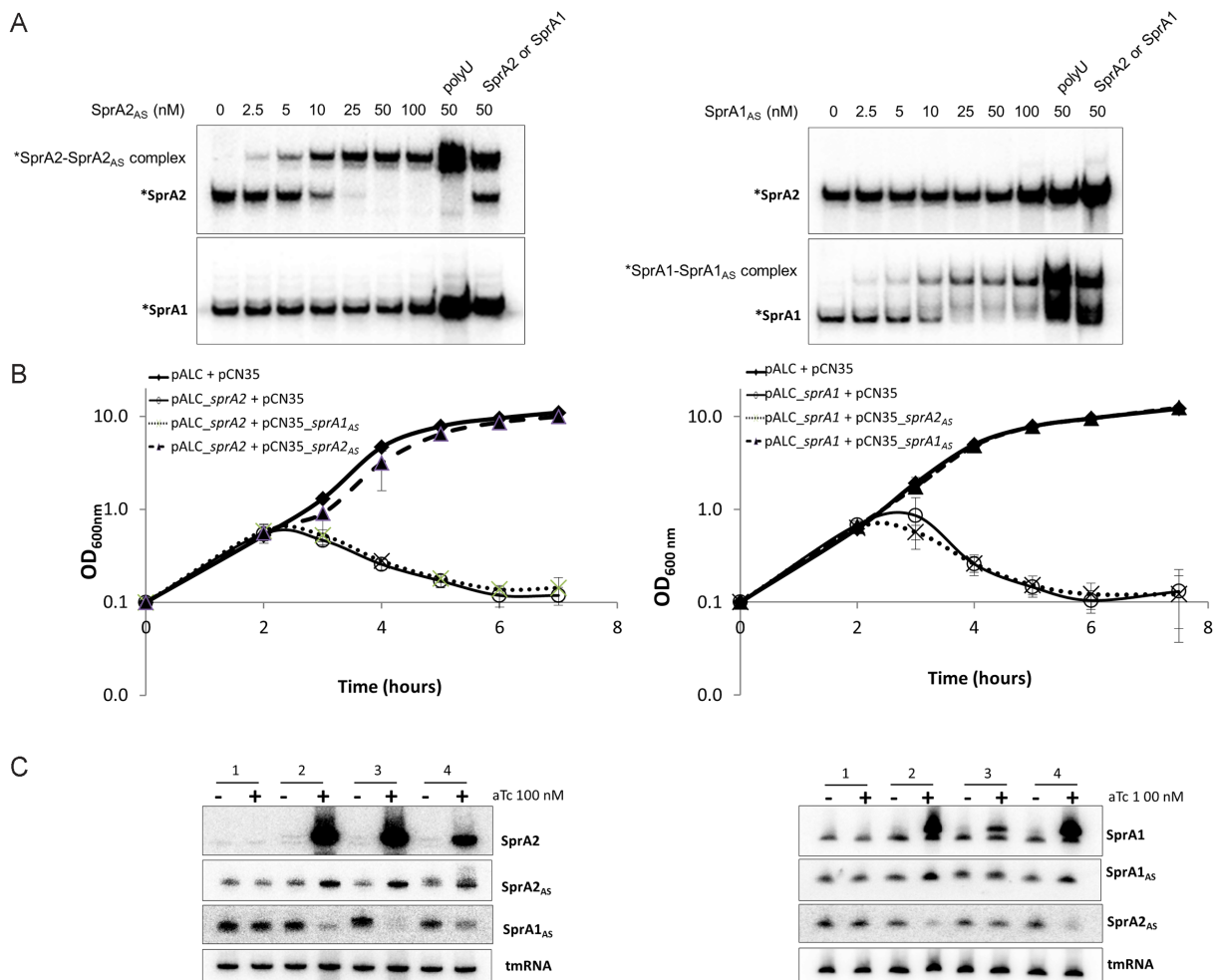


Figure 8. SprA2/SprA2_{AS} and SprA1/SprA1_{AS} pairs act independently. (A) Native gel shift assays of purified labelled SprA2 and SprA1 toxins with increasing amounts of (left) unlabelled SprA2_{AS} or (right) SprA1_{AS} antitoxins. To assess complex specificity, 200 nM of either toxin's RNA or 2 μ M polyuridine (polyU) RNA was added. (B) Comparative growth curves to assess the antitoxin roles of SprA1_{AS} and SprA2_{AS}. Cells were grown for 2 h, after which 100 nM anhydrotetracycline (aTc) was added to overexpress the Pep toxins. Shown are *Staphylococcus aureus* Newman strains containing (left) empty plasmids pALC + pCN35 (squares); pALC_{sprA2} + pCN35 (circles); pALC_{sprA2} + pCN35_{sprA1AS} (crosses); or pALC_{sprA2} + pCN35_{sprA2AS} (triangles); or (right) empty plasmids pALC + pCN35 (squares); pALC_{sprA1} + pCN35 (circles); pALC_{sprA1} + pCN35_{sprA1AS} (triangles); or pALC_{sprA1} + pCN35_{sprA2AS} (crosses). (C) RNA expression profiles after 30 min of aTc induction. Shown are *S. aureus* Newman strains containing: (left) pALC + pCN35; pALC_{sprA2} + pCN35; pALC_{sprA2} + pCN35_{sprA1AS}; and pALC_{sprA2} + pCN35_{sprA2AS}, listed as 1–4, respectively; and (right) pALC + pCN35; pALC_{sprA1} + pCN35; pALC_{sprA1} + pCN35_{sprA1AS}; and pALC_{sprA1} + pCN35_{sprA2AS}, listed as 1–4, respectively. tmRNA was used as the loading control.

detected with 30 pmol of 3' SprA2_{AS}, whereas strong inhibition was already observed using the same amount of 5' SprA2_{AS} (Figure 7C). Moreover, SprA2_{AS} binds its target with high affinity: its apparent K_d of 13 nM is similar to the 15 nM observed for the SprA1/SprA1_{AS} TA system, and is slightly higher than the >1 nM value for SprG1/SprF1 (17,20). Our in-depth characterization of the mechanism involved indicates that SprA2 overexpression (and therefore PepA2 expression) has no effect on the activity of the P_{sprA2_{as}} promoter, but it increases the stability of the antitoxin by nine, presumably due to its titration by SprA2 and an enhanced stability of the complex.

In the present work, we investigated whether cross-regulation occurs between SprA1/SprA1_{AS} and SprA2/SprA2_{AS} type I TA modules. Instances of crosstalk are largely under documented (31,32). To our knowledge,

so far crosstalk has only been reported in other bacteria for one type II TA system (33) and also elegantly between a type I and a type II TA system (34) and between a type II and type V TA system (35). Here, our *in vivo* and *in vitro* analyses showed that when it comes to toxicity regulation, the antitoxins involved are specific to their cognate modules. Moreover, we showed that the SprA2_{AS} antitoxin responds to an osmotic shock and to nutrient starvation, whereas previous studies conducted on the SprA1/SprA1_{AS} TA system revealed that PepA1 expression increased upon oxidative and acidic stresses due to a decrease in antitoxin levels (18). Both studies indicate that the key factor for allowing or repressing PepA1 or PepA2 expression is the corresponding antitoxin RNA level. PepA2 shares 50% amino acid identity with PepA1 (Supplementary Figure S1). Both of the PepA1 and PepA2

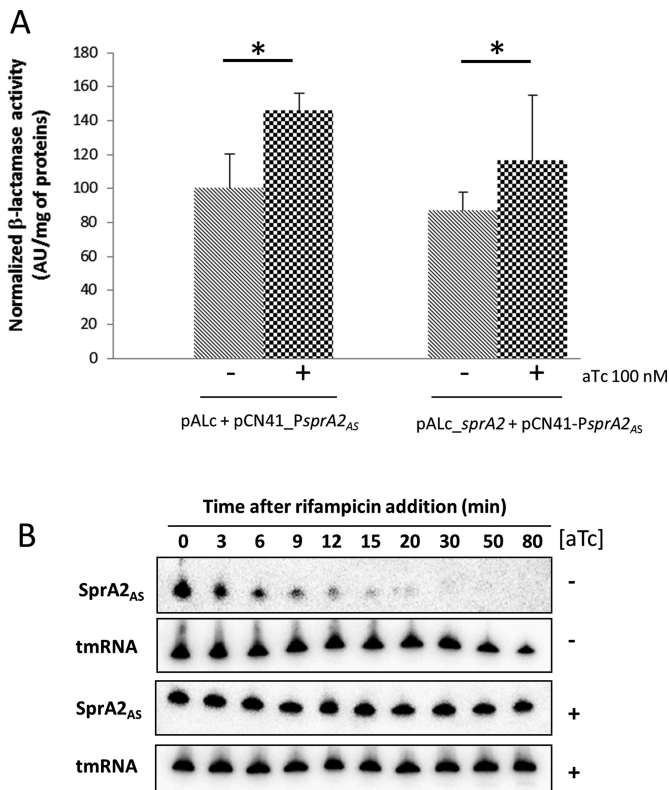


Figure 9. The presence of SprA2 affects SprA2_{AS} stability. (A) The effects of SprA2 on the transcriptional activity of the *SprA2*_{AS} promoter (*PsprA2*_{AS}). *S. aureus* Newman pALC and pALC_{*sprA2*} were co-transformed with pCN41_{*PsprA2*}_{AS}. SprA2 expression was induced with 100 nM anhydrotetracycline (aTc) and β-lactamase activity was measured after 30 min. For each lane, the activity was normalized by subtracting the background signal from the same strain in which pCN41c_{*PsprA2*}_{AS} was replaced by the pCN41 empty vector (not shown). The data presented are the mean of three independent experiments performed in triplicate ± standard deviation. **P* < 0.05 (Mann-Whitney U test). (B) The half-life of SprA2_{AS} increased when SprA2 was overexpressed. *S. aureus* Newman strain with pALC_{*sprA2*} + pCN35_{*sprA2*}_{AS} was grown in brain heart diffusion, then SprA2 expression was induced by 100 nM aTc. After 30 min, 200 μg/ml rifampicin was added to the culture, and total RNAs extracted at different time intervals. tmRNA was used as an internal loading control. The data shown are from one representative experiment out of three performed.

N-terminal domains are rich in hydrophobic aliphatic amino acids that confer hydrophobicity and hemolytic potencies (26,36,37). Such hydrophobic content is also encountered in SprG1, another staphylococcal type I toxin (20) or also in the phenol-soluble modulins (38). Many type I TA systems form pores in bacterial membranes, inducing bacterial death (16,18,38,39). However, in our study, PepA1 and PepA2 exhibit different features. While PepA1 has both antimicrobial and hemolytic activity (17,18,26), our data indicates that PepA2 is mostly cytotoxic, rather than acting very strongly against either Gram-positive and Gram-negative bacteria. PepA2 is about 10 times more effective on human erythrocytes than PepA1 (Figure 5). Our results suggest that PepA2 has a serious potential to damage eukaryotic membranes compared to bacterial membranes, and may belong to *Staphylococcus aureus*

virulence arsenal, along with other leukocidins such as the phenol-soluble modulins (40).

Overall, because of the specificity of each antitoxin to a single RNA and their differences in toxin targets, effectiveness, and responses to various environmental stimuli, we raise the question of their redundancies. Redundancy within TA systems is usually attributed to the fact that deletion of a single TA system was insufficient to confer a significant phenotype (41). TA systems were originally described in post-segregational killing mechanism and to mediate programmed cell death (42), therefore being efficient killers. It was then demonstrated that they could induce stasis (42), and several recent studies have called attention to their role in commitment to persistence through fluctuations in the alarmone (p)ppGpp involved in the stringent response (41). Therefore, TA systems (including type I) have a broad spectrum of action (14,16), and are sometimes difficult to link to a phenotype (43). Here, our data do not pinpoint a specific role for the SprA2/SprA2_{AS} module in bacterial stasis or persistence. Contrary to (42), overexpression of SprA2 led to a sudden growth arrest followed by decreased absorbance measures. This suggests cell death, a conclusion supported after spreading cells on agar plates in the absence of the inducer. Expression levels measured under different stress conditions allowed us to identify a drop in SprA2_{AS} RNA levels in the case of hyperosmotic conditions and during nutrient starvation, which promotes a stringent response. A functional link between SprA2/SprA2_{AS} and (p)ppGpp has not yet been investigated. However, our data does suggest that each TA system has dedicated effectors and roles and must therefore participate in the adaptive response to environmental changes (44–46), possibly including those encountered when in contact with the host during infection or colonization. Indeed, there is growing evidence in recent publications for TA systems that are not linked to persister cell formation (45). In *S. aureus*, the discovery and characterization of type I TA systems is limited to a few studies (8,17,20), all of which involve cell death. In other bacterial and clinical pathogens, type I TA modules have various mechanisms of action, functions, and triggers (14,16,24,47). These include plasmid maintenance, regulation of the SOS response, abortive phage infection, and biofilm formation (48–52). Conversely, more is known about staphylococcal type II TA systems (43). A recent article demonstrated that persister levels were unaffected when all known type II TA systems were knocked out (53). In that study, the authors showed that persister production is critically dependent on the drop in intracellular ATP, and this might be the case for all Gram-positive bacteria. Additionally, studies on the *S. aureus* type II system MazEF pinpointed a possible regulatory relationship with staphylococcal pathogenicity (54). Similarly, the PemIKSa TA system's participation in staphylococcal virulence regulation could be linked to an altered translation of a large set of genes that promote virulence factor expression (55). Finally, the physiological role of SavRS, a novel type II *S. aureus* TA system, was recently described (56). The deletion of this system increased hemolytic activity and pathogenicity in a mouse subcutaneous abscess model. Additionally, the authors showed that the TA system could repress virulence gene expression by direct binding. Ongoing efforts

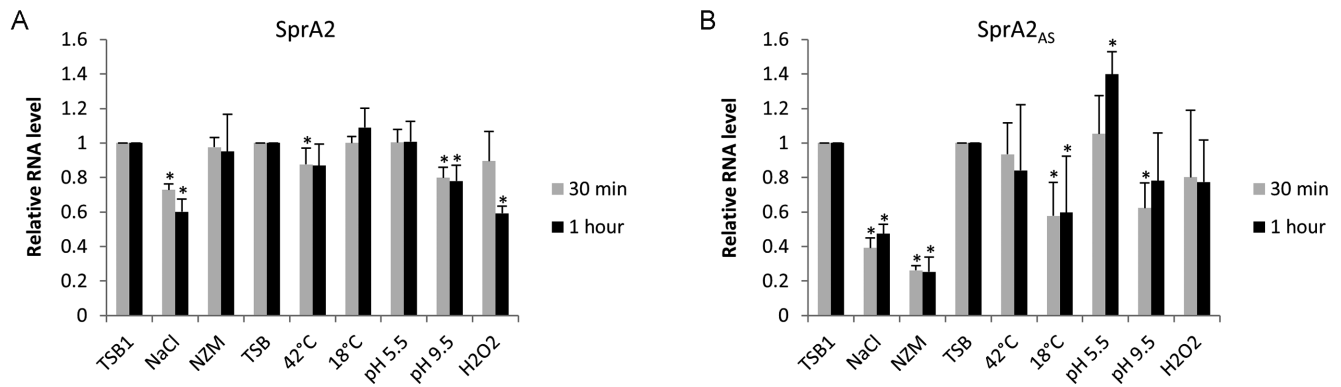


Figure 10. Expression of *SprA2* and *SprA2_{AS}* monitored by northern blots under various stresses. *Staphylococcus aureus* Newman was cultured in tryptic soy broth (TSB) to an OD₆₀₀ of 2, stress applied, then RNA extracted to monitor (A) *SprA2* and (B) *SprA2_{AS}* transcript levels. Stress was induced either by centrifuging bacteria prior to resuspension in appropriate medium, or performed by directly adding the stressor to the growth medium. Pellets were resuspended in fresh TSB (TSB1), TSB supplemented with 1 M NaCl (mimicking osmotic stress), or in NZM medium (emulating a stringent response). Other stresses were induced by adding H₂O₂, HCl or NaOH, or by changing the temperature to 18 or 42°C. The TSB lane corresponds to cells maintained in TSB under normal conditions. The relative expression levels were calculated after quantification of northern blot bands using TSB1 or TSB as calibrators. For all experiments, tmRNA was used as an internal loading control. The data presented are the mean of three independent experiments. Statistical analysis was conducted using the one-tailed Mann–Whitney test; differences were considered statistically significant when $P < 0.05$.

to characterize the different SprFs/SprGs type I TA modules support the hypothesis that each TA system has specific roles. SprG1 is an efficient killer (20), whereas some of the newly characterized SprG toxins induce bacterial stasis and are therefore probably involved in persistence (57). Additionally, studies on the SprGs/SprFs system revealed that they respond to different triggers, and that overexpression of one component does not increase the cognate partner's stability but reduces the cognate's transcript levels. Altogether, recent progress in the study and characterization of staphylococcal type I TA systems, suggest that their biological roles, mode of actions, and redundancies may be reconsidered. Our findings provide novel insights into the roles and functions of such a system. They suggest that, *in vivo*, *S. aureus* may specifically control PepA2 expression to induce cytotoxicity when it is necessary, especially during infection. A tight control of PepA2 expression would therefore be needed to avoid bacterial death internally. Alternately, some clones might behave altruistically by producing PepA2 and undergoing cell death while promoting cytotoxicity, thus guaranteeing the success and fitness of the community.

SUPPLEMENTARY DATA

Supplementary Data are available at NAR Online.

ACKNOWLEDGEMENTS

We thank Stéphane Dréano (IGDR) for DNA sequencing; Michelle Baudy Floc'h and Amor Mosbah for their assistance with chemical synthesis; and Julie Bronsard for sharing total RNAs under stress conditions. We also thank the Biosit flow cytometry platform (Rennes, France). Finally, we thank Camille Riffaud and Marie-Laure Pinel-Marie for helpful discussions and for sharing information regarding the SprG/F TA systems.

Author contributions: N.G.A. performed most of the experiments, along with Y.A., E.C., V.L., I.N. and A.R. Research

was supervised by Y.A., A.R. and B.F. The data was analysed by N.G.A., Y.A., V.L., A.R. and B.F. Figures were prepared by N.G.A. and V.L. Y.A. wrote the manuscript, and it was edited by N.G.A., V.L., I.N., A.R. and B.F.

FUNDING

Marie Curie International Incoming Fellowship [621959-SarHyb to Y.A.] within the European Commission's Seventh Community Framework Programme; Institut National de la Santé et de la Recherche Médicale; the University of Rennes 1; French National Research Agency [sRNA-FIT to B.F.]; Fondation pour la Recherche Médicale [DBF20160635724 to B.F.]. The funders had no role in study design, data collection or analysis, decision to publish, or preparation of the manuscript. Funding for open access charge: Inserm.

Conflict of interest statement. None declared.

REFERENCES

- Anstead, G.M., Cadena, J. and Javeri, H. (2014) Treatment of infections due to resistant *Staphylococcus aureus*. *Methods Mol. Biol.*, **1085**, 259–309.
- Zecconi, A. and Scali, F. (2013) *Staphylococcus aureus* virulence factors in evasion from innate immune defenses in human and animal diseases. *Immunol. Lett.*, **150**, 12–22.
- Felden, B., Vandenesch, F., Bouloc, P. and Romby, P. (2011) The *Staphylococcus aureus* RNome and its commitment to virulence. *PLoS Pathog.*, **7**, e1002006.
- Caldelari, I., Chao, Y., Romby, P. and Vogel, J. (2013) RNA-mediated regulation in pathogenic bacteria. *Cold Spring Harb. Perspect. Med.*, **3**, a010298.
- Fechter, P., Caldeleri, I., Lioliou, E. and Romby, P. (2014) Novel aspects of RNA regulation in *Staphylococcus aureus*. *FEBS Lett.*, **588**, 2523–2529.
- Wagner, E.G. and Romby, P. (2015) Small RNAs in bacteria and archaea: who they are, what they do, and how they do it. *Adv. Genet.*, **90**, 133–208.
- Sassi, M., Augagneur, Y., Mauro, T., Ivain, L., Chabelskaya, S., Hallier, M., Sallou, O. and Felden, B. (2015) SRD: a *Staphylococcus* regulatory RNA database. *RNA*, **21**, 1005–1017.

8. Beaume, M., Hernandez, D., Farinelli, L., Deluen, C., Linder, P., Gaspin, C., Romby, P., Schrenzel, J. and Francois, P. (2010) Cartography of methicillin-resistant *S. aureus* transcripts: detection, orientation and temporal expression during growth phase and stress conditions. *PLoS One*, **5**, e10725.
9. Bronsard, J., Pascreau, G., Sassi, M., Mauro, T., Augagneur, Y. and Felden, B. (2017) sRNA and cis-antisense sRNA identification in *Staphylococcus aureus* highlights an unusual sRNA gene cluster with one encoding a secreted peptide. *Sci. Rep.*, **7**, 4565.
10. Howden, B.P., Beaume, M., Harrison, P.F., Hernandez, D., Schrenzel, J., Seemann, T., Francois, P. and Stinear, T.P. (2013) Analysis of the small RNA transcriptional response in multidrug-resistant *Staphylococcus aureus* after antimicrobial exposure. *Antimicrob. Agents Chemother.*, **57**, 3864–3874.
11. Lasa, I., Toledo-Arana, A., Dobin, A., Villanueva, M., de los Mozos, I.R., Vergara-Irigaray, M., Segura, V., Fagegaltier, D., Penades, J.R., Valle, J. et al. (2011) Genome-wide antisense transcription drives mRNA processing in bacteria. *Proc. Natl. Acad. Sci. U.S.A.*, **108**, 20172–20177.
12. Liu, W., Rochat, T., Toffano-Nioche, C., Le Lam, T.N., Bouloc, P. and Morvan, C. (2018) Assessment of Bona Fide sRNAs in *Staphylococcus aureus*. *Front. Microbiol.*, **9**, 228.
13. Pichon, C. and Felden, B. (2005) Small RNA genes expressed from *Staphylococcus aureus* genomic and pathogenicity islands with specific expression among pathogenic strains. *Proc. Natl. Acad. Sci. U.S.A.*, **102**, 14249–14254.
14. Fernandez-Garcia, L., Blasco, L., Lopez, M., Bou, G., Garcia-Contreras, R., Wood, T. and Tomas, M. (2016) Toxin-Antitoxin systems in clinical pathogens. *Toxins (Basel)*, **8**, 227.
15. Schuster, C.F. and Bertram, R. (2016) Toxin-Antitoxin Systems of *Staphylococcus aureus*. *Toxins (Basel)*, **8**, 140.
16. Brantl, S. and Jahn, N. (2015) sRNAs in bacterial type I and type III toxin-antitoxin systems. *FEMS Microbiol. Rev.*, **39**, 413–427.
17. Sayed, N., Jousselin, A. and Felden, B. (2012) A cis-antisense RNA acts in trans in *Staphylococcus aureus* to control translation of a human cytolitic peptide. *Nat. Struct. Mol. Biol.*, **19**, 105–112.
18. Sayed, N., Nonin-Lecomte, S., Rety, S. and Felden, B. (2012) Functional and structural insights of a *Staphylococcus aureus* apoptotic-like membrane peptide from a toxin-antitoxin module. *J. Biol. Chem.*, **287**, 43454–43463.
19. Brielle, R., Pinel-Marie, M.L. and Felden, B. (2016) Linking bacterial type I toxins with their actions. *Curr. Opin. Microbiol.*, **30**, 114–121.
20. Pinel-Marie, M.L., Brielle, R. and Felden, B. (2014) Dual toxic-peptide-coding *Staphylococcus aureus* RNA under antisense regulation targets host cells and bacterial rivals unequally. *Cell Rep.*, **7**, 424–435.
21. Fozo, E.M., Hemm, M.R. and Storz, G. (2008) Small toxic proteins and the antisense RNAs that repress them. *Microbiol. Mol. Biol. Rev.*, **72**, 579–589.
22. Balaban, N.Q., Gerdes, K., Lewis, K. and McKinney, J.D. (2013) A problem of persistence: still more questions than answers? *Nat. Rev. Microbiol.*, **11**, 587–591.
23. Wagner, E.G. and Brantl, S. (1998) Kissing and RNA stability in antisense control of plasmid replication. *Trends Biochem. Sci.*, **23**, 451–454.
24. Harms, A., Brodersen, D.E., Mitarai, N. and Gerdes, K. (2018) Toxins, targets, and triggers: an overview of toxin-antitoxin biology. *Mol. Cell*, **70**, 768–784.
25. Mauro, T., Rouillon, A. and Felden, B. (2016) Insights into the regulation of small RNA expression: SarA represses the expression of two sRNAs in *Staphylococcus aureus*. *Nucleic Acids Res.*, **44**, 10186–10200.
26. Solecki, O., Mosbah, A., Baudy Floc'h, M. and Felden, B. (2015) Converting a *Staphylococcus aureus* toxin into effective cyclic pseudopeptide antibiotics. *Chem. Biol.*, **22**, 329–335.
27. Busch, A., Richter, A.S. and Backofen, R. (2008) IntaRNA: efficient prediction of bacterial sRNA targets incorporating target site accessibility and seed regions. *Bioinformatics*, **24**, 2849–2856.
28. Helle, L., Kull, M., Mayer, S., Marincola, G., Zelder, M.E., Goerke, C., Wolz, C. and Bertram, R. (2011) Vectors for improved Tet repressor-dependent gradual gene induction or silencing in *Staphylococcus aureus*. *Microbiology*, **157**, 3314–3323.
29. Charpentier, E., Anton, A.I., Barry, P., Alfonso, B., Fang, Y. and Novick, R.P. (2004) Novel cassette-based shuttle vector system for gram-positive bacteria. *Appl. Environ. Microbiol.*, **70**, 6076–6085.
30. Le Pabic, H., Germain-Amiot, N., Bordeau, V. and Felden, B. (2015) A bacterial regulatory RNA attenuates virulence, spread and human host cell phagocytosis. *Nucleic Acids Res.*, **43**, 9232–9248.
31. Iqbal, N., Guerout, A.M., Krin, E., Le Roux, F. and Mazel, D. (2015) Comprehensive functional analysis of the 18 vibrio cholerae N16961 Toxin-Antitoxin systems substantiates their role in stabilizing the superintegron. *J. Bacteriol.*, **197**, 2150–2159.
32. Yoshizumi, S., Zhang, Y., Yamaguchi, Y., Chen, L., Kreiswirth, B.N. and Inouye, M. (2009) *Staphylococcus aureus* YoeB homologues inhibit translation initiation. *J. Bacteriol.*, **191**, 5868–5872.
33. Walling, L.R. and Butler, J.S. (2016) Structural determinants for antitoxin identity and insulation of cross talk between homologous toxin-antitoxin systems. *J. Bacteriol.*, **198**, 3287–3295.
34. Wessner, F., Lacoux, C., Goeders, N., Fouquier d'Herouel, A., Matos, R., Serror, P., Van Melderen, L. and Repoila, F. (2015) Regulatory crosstalk between type I and type II toxin-antitoxin systems in the human pathogen *Enterococcus faecalis*. *RNA Biol.*, **12**, 1099–1108.
35. Wang, X., Lord, D.M., Hong, S.H., Peti, W., Benedik, M.J., Page, R. and Wood, T.K. (2013) Type II toxin/antitoxin MqsR/MqsA controls type V toxin/antitoxin GhoT/GhoS. *Environ. Microbiol.*, **15**, 1734–1744.
36. Chaudhary, K., Kumar, R., Singh, S., Tunkait, A., Gautam, A., Mathur, D., Anand, P., Varshney, G.C. and Raghava, G.P. (2016) A web server and mobile app for computing hemolytic potency of peptides. *Sci. Rep.*, **6**, 22843.
37. Chen, Y., Guarnieri, M.T., Vasil, A.I., Vasil, M.L., Mant, C.T. and Hodges, R.S. (2007) Role of peptide hydrophobicity in the mechanism of action of alpha-helical antimicrobial peptides. *Antimicrob. Agents Chemother.*, **51**, 1398–1406.
38. Brantl, S. (2012) Bacterial type I toxin-antitoxin systems. *RNA Biology*, **9**, 1488–1490.
39. Gurnev, P.A., Ortenberg, R., Dorr, T., Lewis, K. and Bezrukov, S.M. (2012) Persister-promoting bacterial toxin TisB produces anion-selective pores in planar lipid bilayers. *FEBS Lett.*, **586**, 2529–2534.
40. Wang, R., Braughton, K.R., Kretschmer, D., Bach, T.H., Queck, S.Y., Li, M., Kennedy, A.D., Dorward, D.W., Klebanoff, S.J., Peschel, A. et al. (2007) Identification of novel cytolitic peptides as key virulence determinants for community-associated MRSA. *Nat. Med.*, **13**, 1510–1514.
41. Tian, C., Semsey, S. and Mitarai, N. (2017) Synchronized switching of multiple toxin-antitoxin modules by (p)ppGpp fluctuation. *Nucleic Acids Res.*, **45**, 8180–8189.
42. Pedersen, K., Christensen, S.K. and Gerdes, K. (2002) Rapid induction and reversal of a bacteriostatic condition by controlled expression of toxins and antitoxins. *Mol. Microbiol.*, **45**, 501–510.
43. Sierra, R., Viollier, P. and Renzoni, A. (2018) Linking toxin-antitoxin systems with phenotypes: a *Staphylococcus aureus* viewpoint. *Biochim. Biophys. Acta Gene Regulatory Mechanisms*, doi:10.1016/j.bbgrm.2018.07.009.
44. Bukowski, M., Rojowska, A. and Wladyka, B. (2011) Prokaryotic toxin-antitoxin systems—the role in bacterial physiology and application in molecular biology. *Acta Biochim. Pol.*, **58**, 1–9.
45. Curtis, T.D., Takeuchi, I., Gram, L. and Knudsen, G.M. (2017) The influence of the toxin/antitoxin mazEF on growth and survival of *Listeria monocytogenes* under stress. *Toxins (Basel)*, **9**, 31.
46. Gerdes, K., Christensen, S.K. and Lobner-Olesen, A. (2005) Prokaryotic toxin-antitoxin stress response loci. *Nat. Rev. Microbiol.*, **3**, 371–382.
47. Jahn, N. and Brantl, S. (2013) One antitoxin—two functions: SR4 controls toxin mRNA decay and translation. *Nucleic Acids Res.*, **41**, 9870–9880.
48. Patel, S. and Weaver, K.E. (2006) Addiction toxin Fst has unique effects on chromosome segregation and cell division in *Enterococcus faecalis* and *Bacillus subtilis*. *J. Bacteriol.*, **188**, 5374–5384.
49. Vogel, J., Argaman, L., Wagner, E.G. and Altuvia, S. (2004) The small RNA IstR inhibits synthesis of an SOS-induced toxic peptide. *Curr. Biol.*, **14**, 2271–2276.
50. Kawano, M., Aravind, L. and Storz, G. (2007) An antisense RNA controls synthesis of an SOS-induced toxin evolved from an antitoxin. *Mol. Microbiol.*, **64**, 738–754.

51. Pecota, D.C. and Wood, T.K. (1996) Exclusion of T4 phage by the hok/sok killer locus from plasmid R1. *J. Bacteriol.*, **178**, 2044–2050.
52. Domka, J., Lee, J., Bansal, T. and Wood, T.K. (2007) Temporal gene-expression in *Escherichia coli* K-12 biofilms. *Environ. Microbiol.*, **9**, 332–346.
53. Conlon, B.P., Rowe, S.E., Gandt, A.B., Nuxoll, A.S., Donegan, N.P., Zalis, E.A., Clair, G., Adkins, J.N., Cheung, A.L. and Lewis, K. (2016) Persister formation in *Staphylococcus aureus* is associated with ATP depletion. *Nat. Microbiol.*, **1**, 16051.
54. Zhu, L., Inoue, K., Yoshizumi, S., Kobayashi, H., Zhang, Y., Ouyang, M., Kato, F., Sugai, M. and Inouye, M. (2009) *Staphylococcus aureus* MazF specifically cleaves a pentad sequence, UACAU, which is unusually abundant in the mRNA for pathogenic adhesive factor SraP. *J. Bacteriol.*, **191**, 3248–3255.
55. Bukowski, M., Lyzen, R., Helbin, W.M., Bonar, E., Szalewska-Palasz, A., Wegrzyn, G., Dubin, G., Dubin, A. and Wladyka, B. (2013) A regulatory role for *Staphylococcus aureus* toxin-antitoxin system PemIKSa. *Nat. Commun.*, **4**, 2012.
56. Wen, W., Liu, B., Xue, L., Zhu, Z., Niu, L. and Sun, B. (2018) Autoregulation and virulence control by the toxin-antitoxin system SavRS in *Staphylococcus aureus*. *Infect. Immun.*, **86**, e00032–18.
57. Riffaud, C., Pinel-Marie, M.L., Pascreau, G. and Felden, B. (2018) Functionality and cross-regulation of the four SprG/SprF type I toxin-antitoxin systems in *Staphylococcus aureus*. *Nucleic Acids Res.*, doi:10.1093/nar/gky1256.
58. Baba, T., Bae, T., Schneewind, O., Takeuchi, F. and Hiramatsu, K. (2008) Genome sequence of *Staphylococcus aureus* strain Newman and comparative analysis of staphylococcal genomes: polymorphism and evolution of two major pathogenicity islands. *J. Bacteriol.*, **190**, 300–310.
59. Kuroda, M., Ohta, T., Uchiyama, I., Baba, T., Yuzawa, H., Kobayashi, I., Cui, L., Oguchi, A., Aoki, K., Nagai, Y. *et al.* (2001) Whole genome sequencing of methicillin-resistant *Staphylococcus aureus*. *Lancet*, **357**, 1225–1240.
60. Law, J., Buist, G., Haandrikman, A., Kok, J., Venema, G. and Leenhouts, K. (1995) A system to generate chromosomal mutations in *Lactococcus lactis* which allows fast analysis of targeted genes. *J. Bacteriol.*, **177**, 7011–7018.
61. McClelland, M., Sanderson, K.E., Spieth, J., Clifton, S.W., Latreille, P., Courtney, L., Porwollik, S., Ali, J., Dante, M., Du, F. *et al.* (2001) Complete genome sequence of *Salmonella enterica* serovar Typhimurium LT2. *Nature*, **413**, 852–856.
62. Lam, M.M., Seemann, T., Bulach, D.M., Gladman, S.L., Chen, H., Haring, V., Moore, R.J., Ballard, S., Grayson, M.L., Johnson, P.D. *et al.* (2012) Comparative analysis of the first complete *Enterococcus faecium* genome. *J. Bacteriol.*, **194**, 2334–2341.
63. Bateman, B.T., Donegan, N.P., Jarry, T.M., Palma, M. and Cheung, A.L. (2001) Evaluation of a tetracycline-inducible promoter in *Staphylococcus aureus* in vitro and in vivo and its application in demonstrating the role of sigB in microcolony formation. *Infect. Immun.*, **69**, 7851–7857.